Eur. Phys. J. B **41**, 377–382 (2004)
DOI: 10.1140/epjb/e2004-00330-7

THE EUROPEAN PHYSICAL JOURNAL B

An extension to the Wheeler phase-field model to allow decoupling of the capillary and kinetic anisotropies

A.M. Mullis[a]

Institute for Materials Research, University of Leeds, Leeds LS2 9JT, UK

Received 15 October 2004 / Received in final form 16 June 2004
Published online 21 October 2004 –

Abstract. The formulation of the phase-field problem due to Wheeler et al. [Physica D **66**, 243 (1993)] has been adopted and extended as a tool for solidification research by many groups around the World. However, an intrinsic problem of this model is that it couples two physically distinct anisotropies, those associated with the surface energy of the solid-liquid interface and attachment kinetics, into a single anisotropy parameter. In this paper we present a simple extension to the Wheeler model in which we show that introducing a complex form of the anisotropy function allows these two physical parameters to be decoupled.

PACS. 81.10.-h Methods of crystal growth; physics of crystal growth – 81.30.Fb Solidification – 64.70.Dv Solid-liquid transitions

Introduction

One of the most fundamental and all pervasive microstructures produced during the solidification of metals is the dendrite. The dendrite is a prime example of a pattern forming system where complex morphologies arise from initially homogeneous conditions due to the highly non-linear response of the controlling system.

One of the central advances in the ability to predict non steady-state dendritic microstructures has been the advent of phase-field modelling [1,2]. The basis of the technique is the definition of a phase variable (say ϕ) the value of which describes the local phase of the material. By assuming that the interface between phases is diffuse, with a finite width δ, ϕ is made continuous and the governing equations can be written in differential form. In the asymptotic limit that $\delta \to 0$ the sharp interface equations must be recovered, which for pure thermal growth would be

$$\frac{\partial T}{\partial t} = D\nabla^2 T \tag{1}$$

$$cD[\hat{\mathbf{n}}(\nabla T)_l - \hat{\mathbf{n}}(\nabla T)_s] = -Lv_n \tag{2}$$

$$T_i = T_m - \frac{L}{c}dK - \beta v_n \tag{3}$$

where D is the thermal diffusivity, assumed equal in the solid and liquid states, L and c are the latent and specific heats per unit volume respectively, $\hat{\mathbf{n}}$ is the outward pointing unit normal to the interface, v_n is the local interface velocity along $\hat{\mathbf{n}}$, T_m is the equilibrium melting temperature of the solid and the subscripts l and s relate to the solid and liquid states respectively. Equation (2) is simply the balance of heat fluxes across the interface, while equation (3) is the moving interface version of the Gibbs-Thomson equation with local interface temperature, T_i, and local curvature, K. Here, β, is a kinetic coefficient and d is the capillary length, which is given by

$$d = \frac{(\sigma + \sigma'')T_m c}{L^2} \tag{4}$$

where $\sigma(\theta)$ the interfacial energy between the solid and liquid phases, θ is the angle between $\hat{\mathbf{n}}$ and the principal growth direction and differentiation is with respect to θ.

For the case in which both σ and β are isotropic these equations have no steady state solutions. Anisotropy can be introduced by letting

$$d = d(\theta) = d_0(1 - \gamma_d \cos k\theta) \tag{5}$$

and additionally sometimes

$$\beta = \beta(\theta) = \beta_0[1 - \gamma_k \cos k(\theta + \theta_0)]. \tag{6}$$

Here, γ_d and γ_k are the strength of the capillary and kinetic anisotropies respectively, k is a mode number, which for growth in a cubic metal will be 4 and θ_0 is the offset between the directions of the kinetic and capillary anisotropies. The steady-state problem has been studied extensively by the application of boundary integral methods [3–5], often referred to as microscopic solvability theory in this context.

[a] e-mail: a.m.mullis@leeds.ac.uk

The principal prediction of solvability theory is that capillary forces break the Ivantsov degeneracy via the relationship

$$R^2V = \frac{2Dd_o}{\sigma^*} \tag{7}$$

where σ^* is the anisotropy dependent eigenvalue for the problem, which for small Peclet numbers is found to vary as $\sigma^*(\gamma_d) \propto \gamma_d^{7/4}$ in the limit p, $\gamma_d \to 0$, where p is the Peclet number for growth

$$p = \frac{VR}{2D} \tag{8}$$

with V and R being the growth velocity and radius of curvature at the tip.

Phase-field is important in the study of the time dependent problem. There are however, a variety of formulations of the technique, even within the restricted case of a single phase solid growing into its pure undercooled melt [6–10].

The anisotropy required to produce dendritic growth is introduced by making δ and in some cases also a characteristic time-scale, τ, functions of θ [8–10]. Where there is just a single anisotropy parameter based on the length scale δ, this effectively couples the two physically independent anisotropies relating to surface energy and atomic attachment kinetics. Karma and Rappel [11] have demonstrated that a judicious choice for $\tau(\theta)$ allows the magnitudes of γ_d and γ_k to be decoupled. However, other formulations of the phase-field technique have remained popular and, unlike some formulations, the Karma and Rappel model has only recently been extended to solutally based systems. Moreover, the range of types of phase diagram to which it can be applied is more limited than some other formulations of the phase-field problem.

In this paper we present an extension to a formulation of the phase-field technique due to Wang et al. [12] and subsequently developed for dendritic growth by Wheeler et al. [10]. In particular we introduce a complex form of the anisotropy as a route to decoupling γ_d and γ_k. The Wheeler model has been taken up extensively by workers in a number of areas. Recent applications of this model include the study of dendritic shapes at high undercoolings [13] and a model for spontaneous grain refinement [14]. Developments of the basic methodology laid out by Wang et al. include, but are not limited to, an extension to alloy solidification [15], solution with adaptive meshing [16], the inclusion of electric currents through the solidifying material [17] and constrained dendritic growth within a channel [18].

Development of the computational model

The basis of the Wheeler model is a Landau-Ginzberg free energy functional

$$F = \int_\Omega \left[s(e,\phi) + \tfrac{1}{2}\varepsilon^2 (\nabla\phi)^2 \right] d\Omega \tag{9}$$

where $s(e, \phi)$ is an entropy density, e is the internal energy density and ε is a constant. Here, $\phi \equiv 1$ in the liquid and 0 in the solid. Following Wheeler et al. [10] we define reference length and time scales w and w^2/D, and a dimensionless temperature u ($T = T_m + u\Delta T$) giving the transport equation as

$$\frac{\partial u}{\partial \tau} + \frac{30\phi^2}{\Delta}(1 - 2\phi + \phi^2)\frac{\partial \phi}{\partial \tau} = \nabla^2 u. \tag{10}$$

The second term on the left-hand side of equation (10) represents the latent heat associated with the change of state, with Δ being the dimensionless undercooling

$$\Delta = \frac{c\Delta T}{L} = \frac{c(T_m - T)}{L}. \tag{11}$$

The anisotropic phase equation is given by

$$\begin{aligned}\frac{\bar{\varepsilon}^2}{m}\frac{\partial \phi}{\partial \tau} = {} & \phi(1-\phi)\left[\phi - \tfrac{1}{2} + 30\bar{\varepsilon}\alpha\Delta u\phi(1-\phi)\right] \\ & - \bar{\varepsilon}^2\frac{\partial}{\partial x}\left(\eta(\theta)\eta'(\theta)\frac{\partial \phi}{\partial y}\right) + \bar{\varepsilon}^2\frac{\partial}{\partial y}\left(\eta(\theta)\eta'(\theta)\frac{\partial \phi}{\partial x}\right) \\ & + \bar{\varepsilon}^2\nabla\cdot\left(\eta^2(\theta)\nabla\phi\right)\end{aligned} \tag{12}$$

where the quantities in equation (12) are given by Wheeler et al. [10] as

$$\alpha = \frac{\sqrt{2}wL^2}{12c\sigma T_m} \tag{13}$$

$$m = \frac{\sigma T_m}{\beta_0 DL} \tag{14}$$

$$\bar{\varepsilon} = \frac{\delta}{w} \quad . \tag{15}$$

and η is some, as yet unspecified, function of θ which introduces an anisotropy into δ.

It can be shown that, in the limit $\delta \to 0$, the interface temperature is given by [10]

$$u = -\frac{d_0}{c\Delta}\left([\eta(\theta) + \eta''(\theta)]K + \frac{\bar{v}_n}{m[\eta(\theta)]^2}\right) \tag{16}$$

where $\bar{v}_n$ is the dimensionless interface velocity.

The standard form of the function η and indeed the only one considered by Wheeler is

$$\eta(\theta) = 1 + \gamma\cos k\theta. \tag{17}$$

When substituted into equation (16) and expanded to first order this gives

$$u = -\frac{d_0}{c\Delta}[1 - (k^2-1)\gamma\cos k\theta]K - \frac{d_0}{mc\Delta}[1 - 2\gamma\cos k\theta]\bar{v}_n \tag{18}$$

which is of the form of equation (3) with $\beta_0 = d_0/mc\Delta$. Moreover the anisotropies are of the form given by equations (5) and (6) provided $\gamma_d/\gamma_k \approx (k^2-1)/2$. That is the ratio of the capillary to kinetic anisotropy is fixed.

However, the derivation of the interface temperature in the asymptotic limit of $\delta \to 0$ is independent of the

form of η. Consequently, we will now consider a form for η that allows the kinetic and capillary anisotropies to be decoupled. Specifically, we will write

$$\eta(\theta) = 1 + \gamma_r \cos k_r\theta + i\gamma_i \cos k_i(\theta + \theta_i) \qquad (19)$$

where γ_r, γ_i, k_r and k_i are respectively the anisotropies and mode numbers for the real and imaginary parts of η. Clearly, at the end of the computation both the interface width, δ, and the phase variable ϕ must be real, as must all the other physical variables such as the interface temperature. The complex form of η is introduced purely as a device to decouple the magnitudes of the capillary and kinetic anisotropies. Consequently, at the end of each time step the incremental change in ϕ, is forced to be real by discarding the imaginary component of the right-hand side of equation (12).

From equation (16) it can be seen that the capillary terms are of order 1 in η, while the kinetic term is or order 2. Consequently, introducing a complex form of η will leave the capillary term unaltered but will affect the kinetic term. That is, γ_d is a function of γ_r only, while γ_k is a function of both γ_r and γ_i, so that decoupling of the capillary and kinetic anisotropies may be achieved. By substituting the complex form of η into equation (20) and taking the real component, we obtain the kinetic function $\beta(\theta)$ as

$$\beta(\theta) = \left(\frac{d_0}{mc\Delta}\right) \frac{A_r(\theta)}{A_r^2(\theta) + A_i^2(\theta)} \qquad (20)$$

where A_r and A_i are the real and imaginary components of η^2 respectively.

The system of differential equations represented by equations (10) and (12) can be solved using a standard numerical techniques. In the work reported here we have used a semi-implicit ADI finite difference scheme for the transport equation, while the phase equation is solved using an explicit forward Euler scheme.

Validation and properties of the model

Upon expanding equation (20) it can be seen that the term $\cos k_i(\theta + \theta_i)$ always appears raised to the power 2 or above in $\beta(\theta)$. Consequently, in order to achieve four-fold symmetry in γ_k, we set $k_i = 2$ and this is the only value of k_i that has been considered. A straightforward analysis reveals that assigning $\theta_i = 0$ allows the magnitude of γ_k to be increased above the value of 2γ found in the standard Wheeler model, while retaining the default direction. Assigning $\theta_i = \pi/4$ allows the magnitude of γ_k to be reduced below 2γ, including allowing γ_k to take negative values, wherein the maximum in $\beta(\theta)$ is offset by 45° from the maximum in $d(\theta)$. Other values of θ_i, which allow a complete decoupling of $\beta(\theta)$ and $d(\theta)$ in both magnitude and direction are admissible, and are discussed briefly at the end of this section.

Validation of the phase-field model has been conducted against the front tracking model of Ihle [19], in which it is also possible to independently vary γ_d and γ_k. This in turn has been compared with the predictions of solvability theory [20,21]. For the purposes of comparison we have adopted the model parameters used by Ihle, namely $\Delta = 0.45$, $d_0 = 0.03097$ (dimensionless) and $\beta_0 = 1.5485$ (dimensionless), where our characteristic length scale, w, and diffusivity, D, (and hence time scale, τ) have been chosen so as to give the same non-dimensionalisation as that employed by Ihle. Two cases have been compared with the work of Ihle, ($\gamma_d = 0.1$, $\gamma_k = 0.1$) and ($\gamma_d = 0.0$, $\gamma_k = 0.1$). Unfortunately, however, Ihle uses the asymmetric diffusivity approach ($D_s = 0$), whereas we employ the symmetric diffusivity approximation ($D_s = D_l$), the latter being more appropriate to thermal growth, which is the basis of the Wheeler model. Here D_s is the diffusivity in the solid and D_l the diffusivity in the liquid. For this reason it is not possible to compare the dendrite tip radii or velocities predicted by the two model directly as the operating point parameter, σ^*, is known to be a function of the ratio D_s/D_l [22,23]. However, we can still compare the computed Peclet numbers obtained from the two models for the growth process.

For the growth of an isothermal parabolic plate into an isotropic undercooled melt the analytical solution gives

$$\Delta = \sqrt{\pi p_o} e^{p_o} \mathrm{erfc}(\sqrt{p_o}). \qquad (21)$$

With $\Delta = 0.45$ the inverse solution to equation (21) yields $p_o = 0.1353$. Our phase-field model yields values of $p = 0.478p_o$ in the case of $\gamma_d = 0.1$, $\gamma_k = 0.1$ and $p = 0.522p_o$ in the case of $\gamma_d = 0.0$, $\gamma_k = 0.1$. By way of comparison the model of Ihle gives $p = 0.468p_o$ and $p = 0.516p_o$ respectively for these two cases. Given the different computational methodologies employed by these two models we consider that this represents very good agreement. It will also be apparent from the above discussion that the model is capable of simulating fully kinetic dendrites, that is where the dendrite morphology is stabilised solely by the kinetic anisotropy ($\gamma_d = 0$).

Figure 1 shows a sequence of simulations in which the magnitude of γ_k has been varied at fixed γ_d, such that a competition between the capillary and kinetic anisotropy arises. Given appropriate choices for γ_d and γ_k a similar sequence of morphologies can be produced by varying Δ at fixed anisotropy, although here we have chosen to vary the anisotropy. In each frame the capillary anisotropy, with magnitude $\gamma_d = 0.30$ (corresponding to a surface energy anisotropy of 0.02 for a four-fold symmetric system), is directed towards the corners of the bounding box and the kinetic anisotropy towards its sides. With the exception of γ_k all the computational parameters are identical across all the simulations. The thermal Peclet number for growth of the dendrites is $p = 0.14$. No random noise is introduced into the simulations and consequently dendritic side-branching has been artificially suppressed. This has been done to facilitate detailed investigation of the tip morphology. At $\gamma_k = 0$ (a) there are four well-defined primary dendrite arms directed along the capillary direction, no other feature are apparent. As γ_k is increased (b) small doublon like features appear directed along the kinetic direction, although well-developed primary dendrites

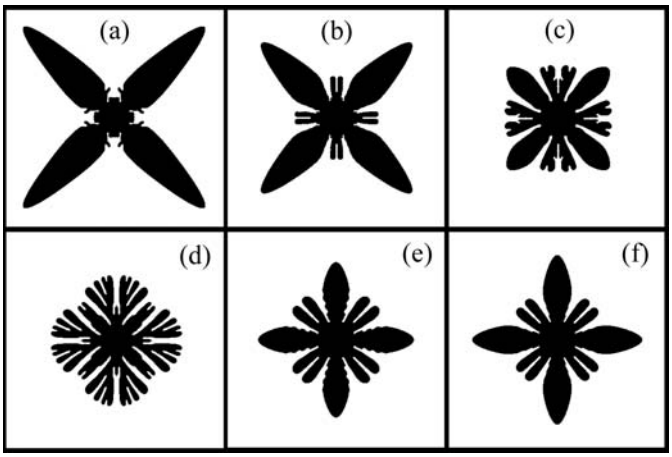

Fig. 1. Sequence of images illustrating the effect of the competition between capillary anisotropy (directed towards the corners of the box) and kinetic anisotropy (directed towards the sides of the box). In all the simulations shown the capillary anisotropy is $\gamma_d = 0.30$. The kinetic anisotropy is (a) $\gamma_k = 0.00$, (b) $\gamma_k = 0.08$, (c) $\gamma_k = 0.14$, (d) $\gamma_k = 0.18$, (e) $\gamma_k = 0.22$ and (f) $\gamma_k = 0.30$. Note that the competition between differently directed anisotropies leads to the formation of structures that are normally associated with low anisotropy systems, such as doublons and dendritic seaweed.

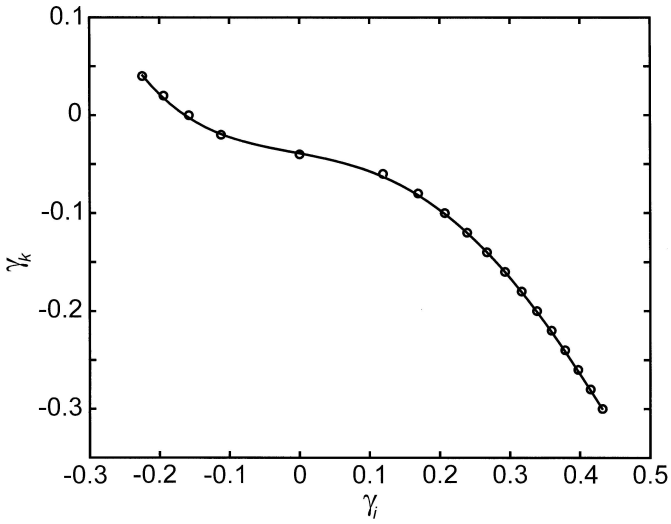

Fig. 2. Relationship between the complex anisotropy parameter γ_i used in the phase-field model and the kinetic anisotropy it generates, γ_k, for the case in which $\gamma_r = 0.02$ and $\theta_i = 0$.

are still apparent along the capillary direction. Further increasing γ_k tends to promote the growth along the direction of the kinetic anisotropy, although the doublon type morphology is now replaced by one more characteristic of 'dendritic seaweed' (c). The capillary dendrites retain their approximately parabolic tip-shape up to the point where the kinetic and capillary growth rates are approximately equal. There then follows a small range in γ_k in which doublon like growth is possible along both the kinetic and capillary directions (d), although this is morphology clearly still favours the kinetic direction. Finally, we see the development of kinetic dendrites (e) with doublon like features along the capillary direction, which eventually reduce in size (f) and disappears with further increases in γ_k. For completeness Figure 2 shows the values of γ_i used to generate values of γ_k up to 0.3. Note however, that because γ_k depend upon both γ_r and γ_i, the values of γ_i shown in Figure 2 apply only to the case in which the value of γ_r is fixed at 0.02.

Finally we deal with the case in which we require an arbitrary offset between the capillary and kinetic anisotropies that is, θ_0 in equation (6) does not take the values 0 or $\pi/4$. This can be accommodated by allowing θ_i to take values other than 0 or $\pi/4$, although because of the non-linear dependence of $\beta(\theta)$ on A_r and A_i it will not in general be the case that $\theta_0 = \theta_i$. However, solving equation (20) for self-consistent values of γ_i and θ_i which yield the desired values of γ_k and θ_0 is a relatively straightforward matter using an iterative least squares algorithm. As an example, say we wish to construct a model in which $\gamma_d = 0.30$ and $\gamma_k = 0.12$, with the additional requirement that the maxima should be offset from each other by $\theta_0 = \pi/8(22.5°)$. As γ_d depends only upon γ_r, we require that $\gamma_r = 0.02$, while $\gamma_i = 0.2906$ and $\theta_i = 0.4650$ rad give the required values of γ_k and θ_0 (≈ 0.3927 rad).

An application of the model - dendrite tip shape

Having developed a model in which γ_d and γ_k can be varied independently, we have proceed to search for general scaling laws relating γ to the operating point parameter σ^* and/or to the dendrite tip shape.

As discussed above, in the asymptotic limit that p, $\gamma_d \to 0$ the well-known result that $\sigma^*(\gamma_d) \propto \gamma_d^{7/4}$ is obtained. A variety of other scaling laws in different asymptotic limits are reported in reference [20], including the limit in which kinetic effects predominate over surface energy, wherein $R \propto \gamma_k^{-5/4}$, independent of the undercooling. The former of these limits is difficult to obtain in the Wheeler formulation of the phase-field method as convergence becomes very slow in the limit of small Δ. However, the later limit is easier to obtain and has been investigated here with $\gamma_d \equiv 0$. The condition for the dominance of kinetics over surface energy is given Brener and Mel'nikov [20] and with $\gamma_d \equiv 0$ can be written in our notation as

$$\frac{\beta_0 V R}{d_0} \gg \left(\frac{1}{\gamma_k}\right)^{1/2}. \tag{22}$$

As shown in Figure 3, the dependence of R upon γ_k has been studied at two values of Δ and excellent agreement with the asymptotic result is obtained. Moreover, the independence of R with changing Δ is also apparent. For the parameters used in this computation the estimated value of $\beta_0 V R/d_0$, measured at $\gamma_k = 0.12$, exceeds $\sqrt{(1/\gamma_k)}$ by a factor of $\approx$250 at $\Delta = 0.34$ and by $\approx$2000 at $\Delta = 0.92$, which we take as satisfying equation (22).

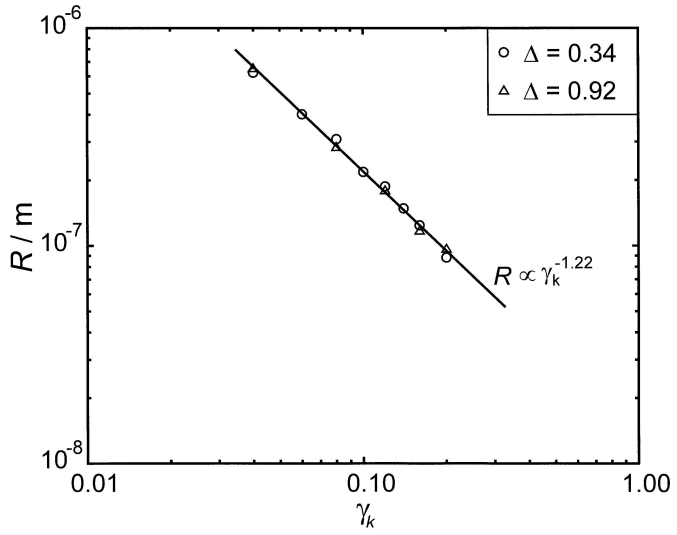

Fig. 3. Dendrite tip radius as a function of γ_k for pure kinetic dendrites ($\gamma_d = 0$) for dimensionless undercoolings of $\Delta = 0.34$ and $\Delta = 0.92$. The least squares regression line shows that there is excellent agreement with the scaling law derived from solvability theory that $R \propto \gamma_k^{-5/4}$ with R independent of Δ.

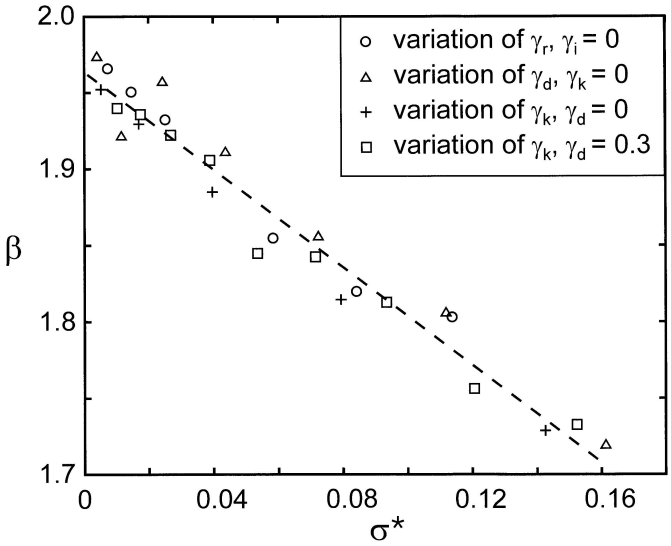

Fig. 4. Dendrite shape parameter, β, as a function of the dimensionless grouping σ^* showing the same linear relationship for pure capillary, pure kinetic and mixed capillary/kinetic dendrites. All results generated at $\Delta = 0.34$.

In the case of isotropic isothermal growth the Ivantsov solution predicts that the dendrite propagates as an exact paraboloid of revolution. However, anisotropy not only breaks the degeneracy in the Ivantsov solution but also acts as a small perturbation to the shape of the dendrite tip. Experimentally, there are a number of techniques for parameterising the shapes of dendrites. In the tip region the most appropriate method is to parameterise the tip as either a low order polynomial [24]

$$z = \sum_{i=1}^{n} a_i x^i \tag{23}$$

or as a power-law

$$z = \alpha \left| x \right|^{\beta}. \tag{24}$$

Clearly, in the former case an exact parabola will result in $a_i \equiv 0$ for $i \neq 2$, while in the later case a value of $\beta \equiv 2$ will be obtained. Here we have used the power-law expressed by equation (24) to parameterise the tip shape as a function of γ in preference to the polynomial formulation. There are two main reasons for this; firstly polynomial fits introduce many additional fitting parameters and secondly the value of the coefficients a_i can depend upon how far back from the dendrite tip the curve fitting is extended [24]. Moreover, for growth in 3-dimensions the physical meaning of the power-law fit parameters α and β is known [25]. There are however physical differences between 2- and 3-dimensional growth, primarily that the in 2-dimensions the dendrite is a good approximation to the Ivantsov parabola along its whole length while in 3-dimensions this is only true near the tip, even in the limit of low anisotropy. Due to these differences the meaning of α and β is less clear in the 2-dimensional case, although it is clear from the results presented below that β does vary in a systematic way with variations in the anisotropy. This variation might also be reflected during 3-dimensional growth, although even if it is not the 2-D results are themselves intrinsically interesting.

In order to study the tip shape as a function of γ the co-ordinates of the dendrite tip (x, z), based on the $\phi = 0.5$ contour, have been extracted up to $2R$ back from the tip. The coefficient β has then been obtained by simple least-squares fitting. We have looked at four systematic variations of γ_r and γ_i and their resultant effect on tip shape:

i. γ_r has been varied with γ_i fixed at zero, this corresponds to the unmodified Wheeler model;
ii. γ_r and γ_i have been varied simultaneously in such a way as to always give $\gamma_k = 0$, this corresponds to pure capillary dendrites;
iii. γ_i has been varied with γ_r fixed at zero, this corresponds to pure kinetic dendrites;
iv. γ_i has been varied with γ_r fixed at a non-zero value (0.02), this corresponds to variation of the kinetic component of the anisotropy with fixed but non-zero capillary anisotropy. In this case the direction of γ_k has been varied so that it both reinforces and opposes the capillary anisotropy.

In presenting the results we have attempted to look for some common scaling of β which is independent of the exact combination of γ_r and γ_i. From Figure 4 it can be seen that one way in which this can be achieved is by plotting β against $\sigma^* = 2Dd_o/R^2V$, wherein a linear trend is observed which is independent of which combination of anisotropies are used to obtain the value of σ^*. In some respects such a scaling may not appear surprising. As discussed above anisotropy provides a small correction to the dendrite shape and consequently a scaling in which the shape parameter β scales varies with σ^* would seem quite

reasonable. However, while σ^* is a useful non-dimensional grouping for capillary dendrites, it would normally be consider far less meaningful for pure kinetic dendrites, primarily because it is R that is constant with undercooling not R^2V. Despite this though it is clear that, at fixed undercooling, a simple scaling between σ^* and β exists for pure capillary, pure kinetic and mixed capillary/kinetic dendrites.

Summary and conclusions

We have presented above straightforward modification to the Wheeler formulation of the phase-field model that allows the magnitudes of the capillary and kinetic anisotropies, γ_d and γ_k, to be decoupled. While there are other formulations of the phase-field problem that also allow this independent variation of γ_d and γ_k many groups around the World have adopted the Wheeler model and new publications based on the application of this model appear on a regular basis. The main advantage of the computational modification proposed here is that it can be very easily accommodated into existing implementations of the Wheeler model, thus protecting the investment in time of those researchers who have implemented and subsequently developed and extended the Wheeler equations.

References

1. J.S. Langer, in *Directions in condensed matter physics* edited by G. Grinstein, G. Mazenko (World Science, 1986), pp. 164-186
2. J.B. Collins, H. Levine, Phys. Rev. B **31**, 6119 (1985)
3. D.A. Kessler, J. Koplik, H. Levine, Adv. Phys. **37**, 255 (1988)
4. Y. Pomeau, M. Ben-Amar, in *Solids far from equilibrium* (Cambridge University Press, 1992), pp. 365-431
5. E. Brener, D. Temkin, Phys. Rev. E **51**, 351 (1995)
6. G. Caginalp, Phys. Rev. A **39**, 5887 (1989)
7. O. Penrose, P.C. Fife, Physica D **43**, 44 (1990)
8. A. Karma, W.J. Rappel, Phys. Rev. Lett. **77**, 4050 (1996)
9. R. Kobayashi, Physica D **63**, 410 (1993)
10. A.A. Wheeler, B.T. Murray, R.J. Schaefer, Physica D **66**, 243 (1993)
11. A. Karma, W.J. Rappel, Phys. Rev. E **53**, R3017 (1996)
12. S.-L. Wang, R.F. Sekerka, A.A. Wheeler, B.T. Murray, S.R. Coriell, R.J. Braun, G.B. McFadden, Physica D **69**, 189 (1993)
13. R. Gonzalez-Cinca, Physica A **414**, 284 (2002)
14. A.M.Mullis, R.F. Cochrane, Acta Mater. **49**, 2205 (2001)
15. J.A. Warren, W.J. Boettinger, Acta Metall. Mater. **43**, 689 (1995)
16. R.J. Braun, B.T. Murray, J. Cryst. Growth **174**, 41 (1997)
17. L.N. Brush, J. Cryst. Growth **247**, 587 (2003)
18. F. Marinozzi, M. Conti, U. Marini Bettolo Marconi, Phys. Rev. E **53**, 2039 (1996)
19. T. Ihle, Eur. Phys. J. B **18**, 337 (2000)
20. E.A. Brener, V.I. Mel'nikov, Adv. Phys. **40**, 53 (1991)
21. Y. Saito, T. Sakiyama, J. Cryst. Growth. **128**, 224 (1993)
22. A. Barbieri, J.S. Langer, Phys. Rev. A, **39**, 5314 (1989)
23. A.M. Mullis, Phys. Rev. E. **68**, 011602 (2003)
24. U. Bisang, J.H. Bilgram, Phys. Rev. E **54**, 5309 (1996)
25. E. Brener, Phys. Rev. Lett. **71**, 3653 (1993)